

A Series of [Mn₆] Complexes with Terminal Functional GroupsMałgorzata Hołyńska*^[a] and Stefanie Dehnen*^[a]**Keywords:** Polynuclear complexes; Manganese; Salicylaldoxime; X-ray diffraction

Abstract. A series of [Mn₆O₂(R¹OH)₄(sao)₆(R²COO)₂] complexes with terminal functional groups (**1**: R¹ = CH₃, R² = HO-C₆H₄, **2**: R¹ = C₂H₅, R² = H₂N-C₆H₄, **3**: R¹ = CH₃, R² = Cl-C₆H₄, **4**: R¹ = CH₃, R² = CH₃-C₆H₄, **5**: R¹ = CH₃, R² = I-C₆H₄, **6**: R¹ = CH₃, R² = pymSCH₂, **7**: R¹ = CH₃, R² = *ortho*-pyr-SCH₃, **8**: R¹ = C₂H₅, R² = (CH₃)₃OOCNHCH₂C₆H₄; sao = doubly deprotonated salicylaldoxime ligand, pym = pyrimidyl, pyr = pyridyl) have been obtained in a reaction of a ligand R²C₆H₄COOH, salicylaldoxime, manganese(II) perchlorate and

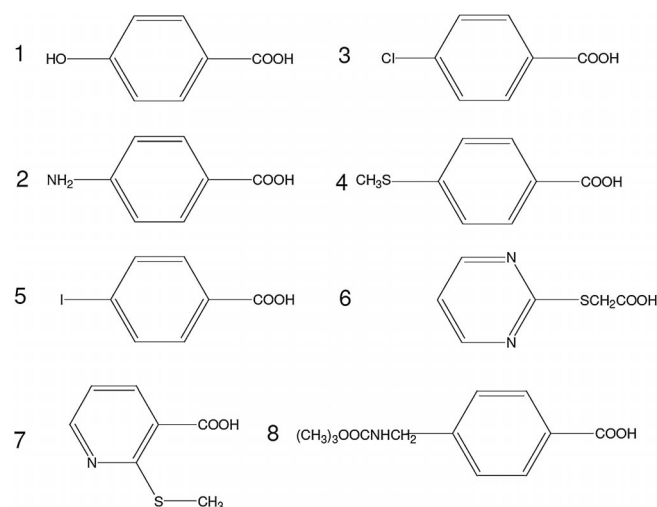
[NEt₄](OH) in methanol or a 1:1 mixture of ethanol and dichloromethane. In this report, structural aspects as well as preliminary studies of magnetic and thermal properties are presented. Compounds **1**, **3**, **6**, **8** exhibit an antiferromagnetic coupling of the Mn²⁺ ions, whereas **4** and **7** show ferromagnetic interactions. The title compounds may act as starting materials for further derivatization addressing the functional groups.

Introduction

Polynuclear mixed-valent manganese complexes represent an established part of materials science. Since the discovery of the first polynuclear mixed-valence [Mn₁₂] complex^[1] exhibiting the so-called “single molecule magnet (SMM) behavior”^[2] attempts have been made to modify the structure of this complex or to create new structural types. An important part of motivation for exploring the chemistry of the ligand part of functionalized SMMs involves the perspective of to attach these molecules to functionalized surfaces via organic reactions.^[3]

New approaches aiming at their assembling into novel frameworks are also worth pursuing, representing part of a “bottom-up” approach.^[4] One possible way into the desired direction would be the functionalization of large metal clusters, which is an uncommon approach in synthetic chemistry, recently utilized for chalcogenidometallates.^[5] It has been shown, that the synthetic principle of introducing functional groups to larger clusters, is of crucial importance for the design of new materials, in particular bearing applications as labeling and imaging agents for biological systems.^[6a] The principle has been especially applied to polyoxoanions of vanadium, molybdenum and tungsten so far.^[6] In this paper we communicate a series of functionalized complexes with a known [Mn₆O₂] core^[7] that was recently published as a complex comprising a record anisotropy barrier for a SMM: [Mn₆O₂(R¹OH)₄(sao)₆(R²COO)₂] (**1**: R¹ = CH₃, R² = HO-C₆H₄, **2**: R¹ = C₂H₅,

R² = H₂N-C₆H₄, **3**: R¹ = CH₃, R² = Cl-C₆H₄, **4**: R¹ = CH₃, R² = CH₃-C₆H₄, **5**: R¹ = CH₃, R² = I-C₆H₄, **6**: R¹ = CH₃, R² = pym-SCH₂, **7**: R¹ = CH₃, R² = *ortho*-pyr-SCH₃, **8**: R¹ = C₂H₅, R² = (CH₃)₃OOCNHCH₂C₆H₄; sao = doubly deprotonated salicylaldoxime, pym = pyrimidyl, pyr = pyridyl). Compounds **1–8** contain sterically well available functional groups (Scheme 1).



Scheme 1. Formulae of acids that served as ligand sources for the ligands bearing functional groups in **1–8**.

Results and Discussion

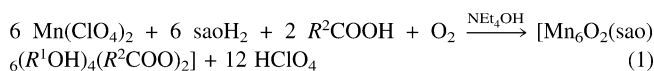
Synthesis

The formation of the **1–8** took place according to equation (1):

* Prof. Dr. S. Dehnen, Dr. M. Hołyńska
E-Mail: dehnen@chemie.uni-marburg.de

[a] Fachbereich Chemie
Wissenschaftliches Zentrum für Materialwissenschaften
Philipps-Universität Marburg
Hans-Meerwein-Strasse
35043 Marburg, Germany

Supporting information for this article is available on the WWW under <http://dx.doi.org/10.1002/zaac.201100524> or from the author.



(1: $R^1 = \text{CH}_3$, $R^2 = \text{HO-C}_6\text{H}_4$, 2: $R^1 = \text{C}_2\text{H}_5$, $R^2 = \text{H}_2\text{N-C}_6\text{H}_4$, 3: $R^1 = \text{CH}_3$, $R^2 = \text{Cl-C}_6\text{H}_4$, 4: $R^1 = \text{CH}_3$, $R^2 = \text{CH}_3\text{S-C}_6\text{H}_4$, 5: $R^1 = \text{CH}_3$, $R^2 = \text{I-C}_6\text{H}_4$, 6: $R^1 = \text{CH}_3$, $R^2 = \text{pym-SCH}_2$, 7: $R^1 = \text{CH}_3$, $R^2 = \text{ortho-pyr-SCH}_3$, 8: $R^1 = \text{C}_2\text{H}_5$, $R^2 = (\text{CH}_3)_3\text{-OOCNHCH}_2\text{-C}_6\text{H}_4$; sao = doubly deprotonated salicylaldoxime ligand, pym = pyrimidyl, pyr = pyridyl).

Crystal Structures

Compounds **1–8** (Figure 1) contain a known $[\text{Mn}_6]$ core,^[7] comprising two $[\text{Mn}_3\text{O}]$ triangles with three Mn^{III} atoms and two μ_3 -bridging oxido ligands, which are linked by two further oxygen atoms from oxime groups. The two subunits are related by a crystallographic symmetry center (Figure 1). Each $[\text{Mn}_3]$ unit also contains three doubly deprotonated salicylaldoxime ligands that surround the three Mn^{III} atoms as a ring of chelating ligands to form a $[\text{MnNO}_3]$ nine-membered ring. One Mn^{III} atom per subunit (Mn1) is pentacoordinate. The second Mn^{III} atom (Mn2) is hexacoordinate as a consequence of additional coordination by the bridging oxygen atom from the opposite subunit. The remaining Mn^{III} atom (Mn3) is hexacoordinate with two solvent molecules (methanol/ethanol) coordinating *trans* to each other. The $R^2\text{-COO}$ ligand coordinates bidentately to the Mn2 and Mn1 (or symmetry equivalent) atoms of each triangular $[\text{Mn}_3]$ unit, in a symmetric μ_2, η_2 -coordination mode. The $\mu_3\text{-O}$ ligand within the triangular $[\text{Mn}_3]$ units is shifted from the $[\text{Mn}_3]$ plane by a minimum value of 0.128(3) Å (in **8**) to a maximum value of 0.232(5) Å (in **1**). (Table S3). All complex molecules in **1–8** differ slightly in the distortion of the $[\text{Mn}_6(\text{sao})_6]$ core, and compounds **2**, **3**, **6** and **7** additionally contain two symmetry-independent molecules that differ in angular distortion of the $[\text{Mn}_3]$ units and the degree of disorder (Table S1).

In all structures, each manganese atom can be unambiguously assigned a formal +3 oxidation state. This is supported by a bond length analysis, clearly revealing the expected Jahn–Teller distortions (Table S1), by BVS calculations (Table S2), and by additional agreement with magnetic properties and EPR spectra. The most obvious difference in the eight title compounds is found in the ligand shell, containing different functional groups, which affect the packing of the molecules in the crystal structures. Whereas the ligands observed in compounds **1–4** were previously reported as ligands to other manganese complexes, as outlined below, the ligands used for the syntheses and stabilization of **5–8** have no precedence in manganese chemistry so far. The 4-hydroxybenzoate ligand in **1** (Figure 1), is mainly known in manganese(II) complexes.^[8] Two cases with Mn^{III} atoms are known,^[8a,b] not exceeding the nuclearity of two. The complex molecules in **1** aggregate into chains extending along [101] (Figure 2, Table S1) via $\text{O-H}\cdots\text{O}$ hydrogen bonds; hydroxyl groups from 4-hydroxybenzoate act as donors and oxygen atoms from coordinating oxime groups act as acceptors. The chains are interconnected by hydrogen

bonds involving solvent water molecules. Compound **2** (Figure 1) contains the 4-aminobenzoate ligand. Recently, *Kozoni et al.*^[9] reported a complex analogous to **2** with 2-hydroxyethanone oxime instead of salicylaldoxime ligands. Here, the same molecules were also observed with two water ligands instead of two methanol ligands, resulting in a novel twist conformation of the complex. In **2**, only one kind of complex is present that adopts the “untwisted” form – as all compounds reported herein. Hydrogen-bonded layers are observed parallel to (011) (Figure S1). Solvent ethanol molecules link the complexes to stabilize the layers. The 4-chlorobenzoate ligand attached to the complex in compound **3** (Figure 1) was previously used for the stabilization of other polynuclear, mixed-valent manganese complexes structures (see for instance^[10]). In **3**, the disordered molecules and solvent molecules are linked via hydrogen bonds to form chains parallel to the crystallographic *a* axis (Figure S1). The ordered molecules do not participate in this interaction, but they are also hydrogen-bonded to disordered solvent molecules. Compound **4** (Figure 1) represents the second known polynuclear manganese complex with the ligand 4-(methylthio)benzoate. The reported SMM $[\text{Mn}_{12}]$ complex was deposited on gold surfaces.^[3] In compound **4**, methanol solvent molecules are hydrogen-bonded to the complex molecules. The complex molecules are packed in columns parallel to the crystallographic *b* axis (Figure S1). They show only weak $\text{C-H}\cdots\pi$ and $\text{C-H}\cdots\text{O}$ interactions and are thus not involved in any supramolecular aggregation. Compound **5** (Figure 1) is the first manganese complex comprising a 4-iodobenzoate ligand. Although **3** and **5** are highly related and triclinic, they are not isomorphous. Complex molecules in **5** form columns along [011] (Figure S1), in which adjacent molecules and disordered methanol molecules are involved in a hydrogen bonding network. The (2-pyrimidylthio)acetate ligand in **6** (Figure 1) has also not been used in manganese chemistry so far, but is rather known from tin(IV) complexes (see for instance^[11a]). Three further examples include a lanthanum complex,^[11b] a silver complex^[11c] and a copper complex.^[11d] Two kinds of hydrogen-bonded chains extending along [010] may be distinguished in **6**. One shows interactions via $\text{O-H}\cdots\text{N}$ hydrogen bridges with methanol O141 atoms as donor and pyrimidyl N261 atoms at $-x, -y + 2, -z$ as acceptors (Table S3). The second is generated by $\text{O-H}\cdots\text{O}$ hydrogen bonds with methanol ligands as both donors and acceptors, as well as solvent methanol molecules as donors to form ring motifs.

Compound **7** (Figure 1) represents the first manganese complex with the 2-(methylthio)nicotinate ligand, which is mainly known from copper(II) chemistry (see for instance^[12]). The complex molecules in **7** are arranged in layers parallel to (101), also stabilized by a hydrogen bonding network (Table S3). Compound **8** (Figure 1) contains the BOC-aminomethylbenzoate ligand which has no precedence in any deposited crystal structure so far. Disordered ethanol ligands that are bonded to Mn3 and are hydrogen-bonded to the oxime O12 atom, whereas the ordered ethanol ligand at Mn3 participates in intermolecular hydrogen bonds, as the complexes interact via $\text{N-H}\cdots\text{O}$ and $\text{O-H}\cdots\text{O}$ hydrogen bonds (Table S3) to form chains extending along [100] (Figure S1).

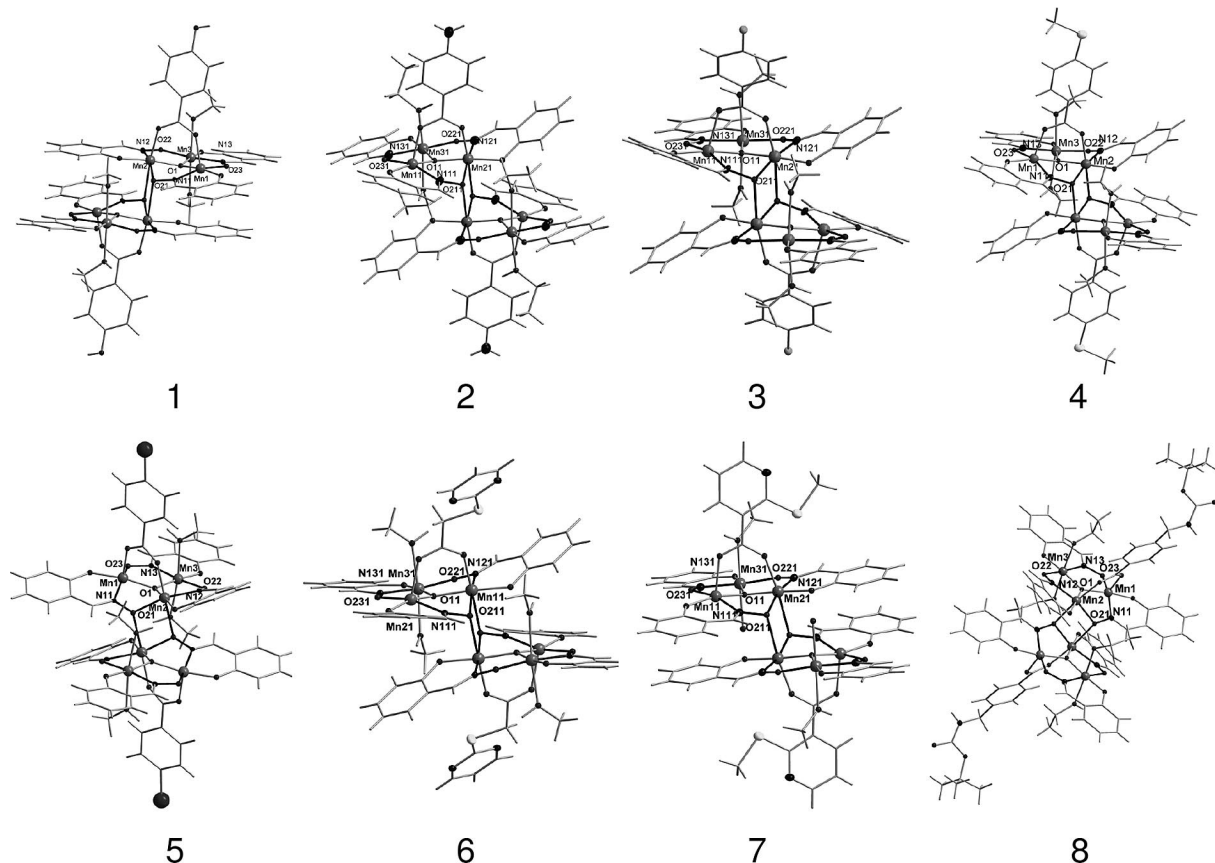


Figure 1. Molecular structures of **1–8** (one symmetry-independent molecule in the case of **2, 3, 6, 7**). The [Mn₆O₂] core is highlighted and an atom labeling scheme is provided for the symmetry independent part of the [Mn₆O₂] core. Carbon and hydrogen atoms are shown as sticks, the remaining atoms are denoted as spheres of arbitrary radii.

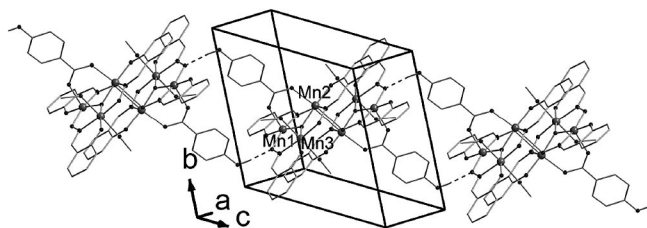


Figure 2. Hydrogen-bonded chains extending along [101] in **1**. Hydrogen bonds are denoted by dashed lines. Only hydrogen atoms involved in hydrogen bonds are shown. The symmetry-independent part of the [Mn₆O₂] core is highlighted.

Preliminary Studies of the Magnetic Properties

The magnetic susceptibility of the title compounds has been examined as a function of the temperature as $\chi T(T)$ at fields of 500, 1000, 5000, or 10000 G, respectively. Also field-dependent measurements have been carried out at 5 and 10 K. Either antiferromagnetic (**1–3, 6, 8**) or ferromagnetic coupling (**4, 5, 7**) of the six metal centers is observed. This seems to be consistent with literature on this class of compounds, where also a variable magnetic behavior is observed and correlated with molecular geometric parameters.^[7] However, some anomalies have been detected, in particular in the case of **2** and **5**, and secondary for **4**, which needs careful checking and a sepa-

rate study. Figure 3 shows the according graphs for **1, 3**, and **6–8** at 500 G.

For **1** the starting value for χT at 295.3 K is 14.82 cm³·mol⁻¹·K⁻¹, thus smaller than expected for six non-interacting Mn^{III} atoms (18.0 cm³·mol⁻¹·K⁻¹), which decreases with decreasing temperature to 5.24 cm³·mol⁻¹·K⁻¹ at about 12 K; then a steep drop at lower temperatures is observed. **8** shows an analogous behavior, starting with χT of 15.84 cm³·mol⁻¹·K⁻¹ at 295.3 K, decreasing smoothly to 7.51 cm³·mol⁻¹·K⁻¹ at 15.50 K and remaining constant to about 14.0 K, followed by a final drop in χT . For **6**, a similar behavior with a more pronounced χT maximum at low temperatures is present. The χT value of **6** decreases from 14.92 cm³·mol⁻¹·K⁻¹ at 295.3 K to 8.09 cm³·mol⁻¹·K⁻¹ at 20.5 K, followed by a small rise to 8.18 cm³·mol⁻¹·K⁻¹ at 13.0 K and then a steep drop. Compound **3** also exhibits antiferromagnetic interactions, but shows modified features with respect to **1** and **6**: the initial χT value at 295.3 K is larger (16.31 cm³·mol⁻¹·K⁻¹), lowering more distinctly to a well-defined minimum of 10.27 cm³·mol⁻¹·K⁻¹ at 29.5 K, followed by a much more pronounced rise to 12.45 cm³·mol⁻¹·K⁻¹ at 6.0 K. The magnetic behavior of compound **7** is different. For **7**, χT amounts to 15.08 cm³·mol⁻¹·K⁻¹ at 295.3 K, similar to the values observed for **1, 3** and **6**, suggesting an antiferromagnetic coupling of the Mn^{III} centers. Also, a decrease upon lowering of the temperature is observed

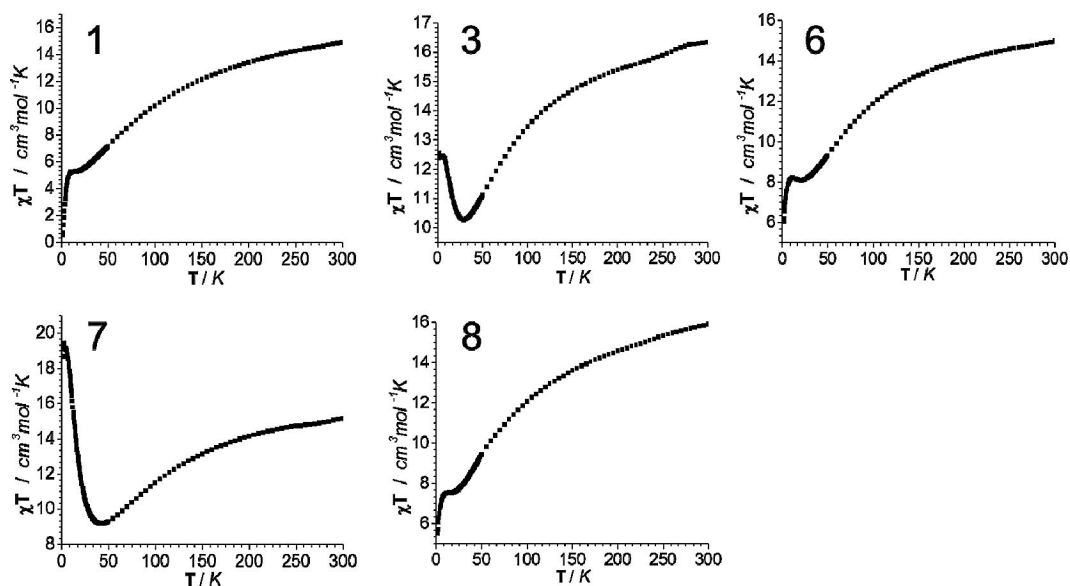


Figure 3. χT vs. T dependencies for **1**, **3**, and **6–8** at 500 G.

to reach $9.17 \text{ cm}^3 \cdot \text{mol}^{-1} \cdot \text{K}^{-1}$ at 42.5 K. However, at even lower temperatures a sudden rise to a sharp maximum of $19.14 \text{ cm}^3 \cdot \text{mol}^{-1} \cdot \text{K}^{-1}$ at 5 K is observed. Compounds **2**, **4** and **5** seem to be unusual in terms of too high/too low χT values. The exploration and understanding of these anomalies are subject to a consecutive study.

The observations described above were compared to the expectations based on the existing reports on oxime-bridged $[\text{Mn}_6]$ complexes. The main idea is that there is a “magic area” of Mn–N–O–Mn torsion angles.^[7] A corresponding value of less than 30.4° should result in antiferromagnetic coupling between the Mn^{III} centers, whereas for values larger than 31.3° , the coupling is expected to be ferromagnetic.^[7] All magnetization field-dependence curves (Figure S4) show a tendency towards saturation, without pronounced hysteresis effects.

Thermal Behavior

The thermal behavior was examined for all title compounds within a broad temperature range. All TG-DSC diagrams with depicted mass losses are shown in the Supporting Information (Figure S6). All compounds, except **4** and **8**, showed a similar general decomposition pattern: before achieving the melting points (**1**: 254, **2**: 215, **3**: 247, **5**: 265, **6**: 206, **7**: 253 °C) a two-step small mass loss is observed, attributable to the release of interstitial solvent (expected as the first step) and of solvent molecules coordinated to manganese centers (expected as the second step). Thus activated material obtained at this step might be useful for further reactions. Upon melting, a multi-step decomposition is observed, with the major step directly following the melting point for **3**, **6** and **7**. For **4** and **8** the stepwise decomposition includes different energetic effects.

Conclusions

A synthetic approach toward eight functionalized mixed-valence polynuclear manganese complexes was shown which

spotlights these compounds with respect to further derivatization and/or linkage. The new materials show either antiferromagnetic or ferromagnetic interactions, essentially in accordance with known magneto-structural correlations. A pronounced effect of intermolecular interactions involving functional groups is visible.

Experimental Section

General: All syntheses were carried out under aerobic conditions. All chemicals were used without further purification. HPLC-grade methanol (HiperSolv Chromanorm, VWR BDH Prolabo) was used. Absolute ethanol purchased from AnalaR NORMAPUR was used. Tetraethylammonium hydroxide (25 % solution in methanol) was purchased from Aldrich and kept under argon. Manganese(II) perchlorate hexahydrate, 4-hydroxybenzoic acid, 4-aminobenzoic acid and 4-chlorobenzoic acid were purchased from Aldrich. 4-(methylthio)benzoic acid and (2-pyrimidylthio)acetic acid were purchased from Acros. Salicylaldehyde was purchased from Merck. 2-(methylthio)nicotinic acid was purchased from Alfa Aesar. 4-(Boc-aminomethyl)benzoic acid was purchased from Fluka. 4-iodobenzoic acid was purchased from Fluorochem. **Caution!** Although no particular problems were faced in case of this work, it should be always taken into consideration that perchlorates are explosive.

Syntheses

[Mn₆O₂(MeOH)₄(sao)₆(HOC₆H₄COO)₂·2(H₂O) (1): 4-hydroxybenzoic acid (0.138 g, 1 mmol), salicylaldehyde (0.137 g, 1 mmol) and manganese(II) perchlorate hexahydrate (0.25 g, 1 mmol) were dissolved in methanol (20 mL) to afford a colorless solution. Subsequently, tetraethylammonium hydroxide (1 mL) was added causing darkening of the mixture. The mixture was stirred for 1 hour. The obtained dark green solution was filtered and left for slow evaporation. Crystals of **1** (dark plates showing red-green pleochroism) formed within 7–10 days in 42 % yield (with respect to salicylaldehyde). **Elemental anal.** calcd. (found) for **1**: C 44.74 (43.83), H 3.75 (3.44), N 5.22 (5.24) %. **IR** (KBr pellet) = 416.1 (m), 466.6 (m), 533.1 (w),

624.8 (s), 649.1 (s), 679.5 (vs), 749.5 (s), 788.4 (w), 827.8 (w), 855.8 (w), 917.5 (vs), 1026.1 (vs), 1098.6 (m), 1124.4 (m), 1153.9 (m), 1170.8 (m), 1202.5 (s), 1277.0 (vs), 1327.8 (w), 1392.5 (vs), 1440.0 (s), 1471.4 (m), 1527.9 (s), 1597.5 (vs), 3392.3 (s) cm⁻¹.

[Mn₆O₂(EtOH)₄(sao)₆(H₂NC₆H₄COO)₂]-1.85(EtOH) (2): of 4-aminobenzoic acid (0.137 g, 1 mmol), salicylaldehyde (0.137 g, 1 mmol) and manganese(II) perchlorate hexahydrate (0.25 g, 1 mmol) were dissolved in a 1:1 mixture of ethanol and dichloromethane (20 mL) to afford a yellow solution. Subsequently, tetraethylammonium hydroxide (1 mL) was added causing darkening of the mixture. The mixture was stirred for 1 hour. The obtained black solution was filtered from yellowish solid and left for slow evaporation. Crystals of **2** (black blocks) formed within 6–10 days in 70% yield (with respect to salicylaldehyde). **Elemental anal.** calcd. (found) for **2**: C 47.19 (46.00), H 4.08 (4.09), N 6.88 (6.98)%. **IR** (KBr pellet) = 416.3 (m), 463.2 (m), 534.3 (w), 648.7 (s), 677.0 (vs), 755.7 (m), 788.9 (w), 823.2 (vw), 852.3 (vw), 915.9 (vs), 1026.4 (vs), 1042.9 (s), 1123.7 (w), 1152.3 (w), 1176.1 (m), 1201.0 (m), 1282.6 (vs), 1325.1 (m), 1384.9 (vs), 1439.6 (s), 1471.1 (m), 1509.9 (s), 1540.9 (s), 1597.2 (vs), 3368.0 (vs) cm⁻¹.

[Mn₆O₂(MeOH)₄(sao)₆(ClC₆H₄COO)₂]-1.33(MeOH)-0.62(H₂O) (3): 4-chlorobenzoic acid (0.156 g, 1 mmol), salicylaldehyde (0.137 g, 1 mmol) and manganese(II) perchlorate hexahydrate (0.25 g, 1 mmol) were dissolved in methanol (20 mL) to afford a colorless solution. Subsequently, tetraethylammonium hydroxide (1 mL) was added causing darkening of the mixture. The mixture was stirred for 1 hour. The obtained dark green solution was filtered and left for slow evaporation. Crystals of **3** (black blocks) formed within 5–8 days in 37% yield (with respect to salicylaldehyde). **Elemental anal.** calcd. (found) for **3**: C 42.31 (41.93), H 3.21 (3.53), N 5.05 (5.13)%. **IR** (KBr pellet) = 463.7 (s), 534.6 (m), 649.1 (vs), 676.7 (vs), 755.3 (s), 826.1 (w), 858.5 (w), 916.2 (vs), 1027.3 (vs), 1043.6 (vs), 1090.4 (w), 1124.0 (w), 1153.3 (w), 1169.4 (w), 1201.4 (m), 1280.7 (vs), 1325.4 (w), 1398.5 (vs), 1439.8 (vs), 1471.2 (m), 1534.5 (vs), 1596.2 (vs), 3399.7 (s) cm⁻¹.

[Mn₆O₂(MeOH)₄(sao)₆(CH₃SC₆H₄COO)₂]-5.37(MeOH) (4): 4-(methylthio)benzoic acid (0.172 g, 1 mmol), salicylaldehyde (0.137 g, 1 mmol) and manganese(II) perchlorate hexahydrate (0.25 g, 1 mmol) were dissolved in methanol (20 mL) to afford a colorless solution. Subsequently, tetraethylammonium hydroxide (1 mL) was added causing darkening of the mixture. The mixture was stirred for 1 hour. The obtained black solution was filtered from greenish solid and left for slow evaporation. Crystals of **4** (black blocks) formed within 5–8 days in 42% yield (with respect to salicylaldehyde). **Elemental anal.** calcd. (found) for **4**: C 44.78 (43.11), H 4.54 (5.41), N 4.65 (5.49), S 3.55 (2.45)%. **IR** (KBr pellet) = 462.2 (s), 531.5 (s), 650.2 (vs), 678.3 (vs), 751.8 (s), 777.3 (m), 824.5 (w), 854.7 (w), 915.8 (vs), 957.3 (w), 1026.7 (vs), 1043.7 (vs), 1091.3 (m), 1123.2 (m), 1151.7 (m), 1185.1 (m), 1200.8 (s), 1278.7 (vs), 1326.7 (m), 1396.5 (vs), 1440.1 (vs), 1470.5 (s), 1523.1 (vs), 1541.6 (s), 1597.0 (vs), 3414.1 (vs) cm⁻¹.

[Mn₆O₂(MeOH)₄(sao)₆(I-C₆H₄COO)₂]-4.7(MeOH) (5): 4-iodobenzoic acid (0.248 g, 1 mmol), salicylaldehyde (0.137 g, 1 mmol) and manganese(II) perchlorate hexahydrate (0.25 g, 1 mmol) were dissolved in methanol (20 mL) to afford a colorless solution. Subsequently, tetraethylammonium hydroxide (1 mL) was added causing darkening of the mixture. The mixture was stirred for 1 hour. The obtained black solution was filtered and left for slow evaporation. Crystals of **5** (black needles) formed within 5–8 days in 38% yield (with respect to salicylaldehyde). **Elemental anal.** calcd. (found) for **5**: C 39.96 (37.59), H 3.72 (2.91), N 4.34 (4.34), I 13.12 (12.76)%. **IR** (KBr pellet) = 409.7 (s), 424.6 (s), 464.6 (s), 536.1 (m), 649.1 (s), 680.5 (vs), 752.1 (s), 831.5 (m), 853.9 (w), 916.9 (vs), 1007.1 (s),

1027.6 (vs), 1043.3 (s), 1124.0 (w), 1152.6 (w), 1202.0 (m), 1279.5 (s), 1328.0 (w), 1394.8 (s), 1440.1 (s), 1471.0 (w), 1533.8 (m), 1582.1 (s), 1597.4 (s), 3437.2 (vw) cm⁻¹.

[Mn₆O₂(MeOH)₄(sao)₆(pym-SCH₂COO)₂]-1.85(MeOH) (6): (2-pyrimidylthio)acetic acid (0.109 g, 1 mmol), salicylaldehyde (0.137 g, 1 mmol) and manganese(II) perchlorate hexahydrate (0.25 g, 1 mmol) were dissolved in methanol (20 mL) to afford a yellow solution. Subsequently, tetraethylammonium hydroxide (1 mL) was added causing darkening of the mixture. The mixture was stirred for 1 hour. The obtained black solution was filtered from black solid and left for slow evaporation. Crystals of **6** (brown blocks) formed within 5–8 days in 25% yield (calculated with respect to salicylaldehyde). **Elemental anal.** calcd. (found) for **6**: C 42.41 (41.20), H 3.62 (3.61), N 8.38 (8.34), S 3.84 (3.68)%. **IR** (KBr pellet) = 404.6 (vs), 414.5 (s), 424.2 (s), 463.4 (s), 527.6 (s), 649.7 (vs), 677.8 (vs), 753.7 (s), 824.7 (m), 863.8 (w), 915.5 (vs), 1025.9 (vs), 1124.4 (w), 1153.8 (m), 1200.5 (s), 1285.9 (s), 1327.6 (m), 1381.8 (s), 1439.4 (m), 1471.7 (w), 1546.9 (m), 1569.2 (s), 1569.2 (s), 1598.1 (s), 3377.9 (vw) cm⁻¹.

[Mn₆O₂(MeOH)₂(H₂O)₂(sao)₆(orto-CH₃S-pyr-COO)₂]_{0.75}·2.02(MeOH)·H₂O** (7):** 2-(methylthio)nicotinic acid (0.169 g, 1 mmol), salicylaldehyde (0.137 g, 1 mmol) and manganese(II) perchlorate hexahydrate (0.25 g, 1 mmol) were dissolved in methanol (20 mL) to afford a yellow solution. Subsequently, tetraethylammonium hydroxide (1 mL) was added causing darkening of the mixture. The mixture was stirred for 1 hour. The obtained black solution was filtered and left for slow evaporation. Crystals of **7** (violet needles) formed within 5–8 days in 22% yield (with respect to salicylaldehyde). **Elemental anal.** calcd. (found) for **7**: C 42.79 (40.57), H 3.86 (3.67), N 6.60 (6.60), S 3.78 (3.77)%. **IR** (KBr pellet) = 429.6 (m), 477.8 (s), 530.9 (m), 624.1 (s), 651.9 (s), 679.2 (vs), 752.1 (s), 826.7 (m), 917.4 (vs), 1026.9 (vs), 1041.8 (s), 1096.4 (s), 1153.3 (m), 1201.6 (m), 1283.4 (s), 1325.6 (w), 1376.0 (s), 1396.1 (m), 1440.1 (s), 1470.5 (m), 1536.8 (m), 1560.3 (m), 1582.6 (s), 1597.5 (s), 3001.1 (vw), 3407.9 (vw) cm⁻¹.

[Mn₆O₂(EtOH)₄(sao)₆(Me₃OOCNHCH₂C₆H₄COO)₂] (8): 4-(boc-aminomethyl)benzoic acid (0.125 g, 0.5 mmol), salicylaldehyde (0.137 g, 1 mmol) and manganese(II) perchlorate hexahydrate (0.25 g, 1 mmol) were dissolved in a 1:1 mixture of ethanol and dichloromethane (20 mL) to afford a colorless solution. Subsequently, tetraethylammonium hydroxide (1 mL) was added causing darkening of the mixture. The mixture was stirred for 1 hour. The obtained dark brown solution was filtered and left for slow evaporation. Crystals of **8** (in form of black blocks) were formed within 7–14 days at 48% yield (calculated with respect to salicylaldehyde). **Elemental anal.** Calcd (found) for **8**: C 49.26 (47.01), H 4.46 (4.72), N 6.05 (6.20)%. **IR** (KBr pellet) = 408.3 (m), 418.1 (m), 467.1 (s), 529.7 (m), 676.1 (vs), 750.3 (s), 765.3 (m), 825.5 (w), 873.5 (w), 916.3 (s), 1001.0 (m), 1029.5 (s), 1045.3 (s), 1074.1 (w), 1162.5 (m), 1200.6 (m), 1278.0 (s), 1324.9 (w), 1398.1 (s), 1443.1 (m), 1472.7 (w), 1535.8 (s), 1598.4 (m), 1712.0 (m) cm⁻¹.

Physical Property Measurements: IR spectra were collected with the aid of a Bruker IFS 88 device. EPR spectra were collected for solid samples in quartz tubes at room and at helium temperature by using a Bruker ESP300 device. ESI-MS spectra were collected by means of a Finnigan LTQ-FT spectrometer for acetonitrile solutions of **1–8**. TGA diagrams for samples of **1–8** (**1**: 16.9, **2**: 7.9, **3**: 20.2, **4**: 6.9, **5**: 8.3, **6**: 13.9, **7**: 11.1, **8**: 11.6 mg) were recorded with a NETZSCH STA 409 CD device at temp. range of 25–1450 °C and scanning rate of 1 K·min⁻¹. Preliminary magnetic properties measurements were carried out by using a Quantum Design SQUID Magnetometer for samples of **1–8**

(1: 15.4, 2: 7.4, 3: 35.0, 4: 16.5, 5: 17.7, 6: 13.9, 7: 22.8, 8: 9.8 mg) in gelatine capsule holders at 2–300 K temperature range. The values were accordingly corrected for the sample holder. Four values of external field were applied (500/1000/5000/10000 G). Also field-dependent measurements at 5 K/10 K were carried out. Diamagnetic corrections were introduced using Pascal constants.^[13] Here only selected results are shown. Especially the behavior of **2**, **4**, and **5** seems to be unusual and requires further studies.

X-ray Crystallography: X-ray data were collected at 100(2) K with IPDS2 or IPDS2T diffractometers or at 193(2) K with an IPDS1 diffractometer,^[14] using graphite-monochromatized Mo- K_{α} radiation ($\lambda = 0.71073 \text{ \AA}$). The structures were solved by direct methods and refined on F^2 by full-matrix least-squares methods using the SHELXTL program package.^[15] Crystal data for **1**: ($M = 1610.78 \text{ g}\cdot\text{mol}^{-1}$): triclinic, space group $P\bar{1}$ (no. 2), $a = 11.732(3)$, $b = 11.934(3)$, $c = 12.835(4) \text{ \AA}$, $\alpha = 105.94(3)$, $\beta = 104.59(3)$, $\gamma = 98.04(3)^\circ$, $V = 1629.5(8) \text{ \AA}^3$, $Z = 1$, $D_c = 1.641 \text{ g}\cdot\text{cm}^{-3}$, $\mu = 1.22 \text{ mm}^{-1}$, 13520 reflections measured ($R(\text{int}) = 0.115$), 6806 unique, 2958 with $I > 2\sigma(I)$ and final R values $R1 = 0.066$ [$I > 2\sigma(I)$]; $wR2 = 0.104$ (all data). Crystal data for **2**: ($M = 1714.03 \text{ g}\cdot\text{mol}^{-1}$): monoclinic, space group $P2_1/c$ (no. 14), $a = 19.970(4)$, $b = 27.694(5)$, $c = 13.945(4) \text{ \AA}$, $\beta = 94.20(3)^\circ$, $V = 7692(3) \text{ \AA}^3$, $Z = 4$, $D_c = 1.480 \text{ g}\cdot\text{cm}^{-3}$, $\mu = 1.03 \text{ mm}^{-1}$, 37157 reflections measured ($R(\text{int}) = 0.070$), 15819 unique, 5415 with $I > 2\sigma(I)$ and final R values $R1 = 0.062$ [$I > 2\sigma(I)$]; $wR2 = 0.097$ (all data). Crystal data for **3**: ($M = 1665.42 \text{ g}\cdot\text{mol}^{-1}$): triclinic, space group $P\bar{1}$ (no. 2), $a = 12.742(3)$, $b = 15.080(4)$, $c = 19.081(4) \text{ \AA}$, $\alpha = 88.03(3)$, $\beta = 73.89(3)$, $\gamma = 80.57(3)^\circ$, $V = 3474.6(14) \text{ \AA}^3$, $Z = 2$, $D_c = 1.592 \text{ g}\cdot\text{cm}^{-3}$, $\mu = 1.22 \text{ mm}^{-1}$, 29015 reflections measured ($R(\text{int}) = 0.058$), 14530 unique, 8807 with $I > 2\sigma(I)$ and final R values $R1 = 0.057$ [$I > 2\sigma(I)$]; $wR2 = 0.130$ (all data). Crystal data for **4**: ($M = 1807.33 \text{ g}\cdot\text{mol}^{-1}$): triclinic, space group $P\bar{1}$ (no. 2), $a = 11.090(3)$, $b = 13.772(4)$, $c = 14.838(4) \text{ \AA}$, $\alpha = 116.06(3)$, $\beta = 95.37(3)$, $\gamma = 103.36(3)^\circ$, $V = 1930.8(9) \text{ \AA}^3$, $Z = 1$, $D_c = 1.554 \text{ g}\cdot\text{cm}^{-3}$, $\mu = 1.09 \text{ mm}^{-1}$, 14410 reflections measured ($R(\text{int}) = 0.064$), 6705 unique, 4331 with $I > 2\sigma(I)$ and final R values $R1 = 0.057$ [$I > 2\sigma(I)$]; $wR2 = 0.145$ (all data). Crystal data for **5**: ($M = 1945.13 \text{ g}\cdot\text{mol}^{-1}$): triclinic, space group $P\bar{1}$ (no. 2), $a = 10.443(3)$, $b = 14.607(4)$, $c = 15.124(4) \text{ \AA}$, $\alpha = 117.01(3)$, $\beta = 93.47(3)$, $\gamma = 104.40(3)^\circ$, $V = 1950.2(9) \text{ \AA}^3$, $Z = 1$, $D_c = 1.656 \text{ g}\cdot\text{cm}^{-3}$, $\mu = 1.81 \text{ mm}^{-1}$, 17732 reflections measured ($R(\text{int}) = 0.097$), 6471 unique, 4439 with $I > 2\sigma(I)$ and final R values $R1 = 0.059$ [$I > 2\sigma(I)$]; $wR2 = 0.153$ (all data). Crystal data for **6**: ($M = 1670.93 \text{ g}\cdot\text{mol}^{-1}$): monoclinic, space group $P2_1/c$ (no. 14), $a = 23.702(5)$, $b = 12.399(4)$, $c = 29.701(5) \text{ \AA}$, $\beta = 128.62(3)^\circ$, $V = 6820(3) \text{ \AA}^3$, $Z = 4$, $D_c = 1.627 \text{ g}\cdot\text{cm}^{-3}$, $\mu = 1.22 \text{ mm}^{-1}$, 30616 reflections measured ($R(\text{int}) = 0.043$), 11405 unique, 9280 with $I > 2\sigma(I)$ and final R values $R1 = 0.038$ [$I > 2\sigma(I)$]; $wR2 = 0.097$ (all data). Crystal data for **7**: ($M = 1698.61 \text{ g}\cdot\text{mol}^{-1}$): triclinic, space group $P\bar{1}$ (no. 2), $a = 12.453(3)$, $b = 12.986(3)$, $c = 22.401(4) \text{ \AA}$, $\alpha = 87.16(3)$, $\beta = 80.71(3)$, $\gamma = 72.82(3)^\circ$, $V = 3415.5(13) \text{ \AA}^3$, $Z = 2$, $D_c = 1.656 \text{ g}\cdot\text{cm}^{-3}$, $\mu = 1.23 \text{ mm}^{-1}$, 20192 reflections measured ($R(\text{int}) = 0.104$), 10985 unique, 8555 with $I > 2\sigma(I)$ and final R values $R1 = 0.062$ [$I > 2\sigma(I)$]; $wR2 = 0.202$ (all data). Crystal data for **8**: ($M = 1853.14 \text{ g}\cdot\text{mol}^{-1}$): triclinic, space group $P\bar{1}$ (no. 2), $a = 11.961(3)$, $b = 12.204(3)$, $c = 14.720(4) \text{ \AA}$, $\alpha = 108.94(3)$, $\beta = 92.44(3)$, $\gamma = 93.87(3)^\circ$, $V = 2023.0(9) \text{ \AA}^3$, $Z = 1$, $D_c = 1.521 \text{ g}\cdot\text{cm}^{-3}$, $\mu = 0.99 \text{ mm}^{-1}$, 30333 reflections measured ($R(\text{int}) = 0.098$), 8574 unique, 6228 with $I > 2\sigma(I)$ and final R values $R1 = 0.057$ [$I > 2\sigma(I)$]; $wR2 = 0.151$ (all data). The supplementary crystallographic data CCDC-807708, -807709, -807710, -807711, -807712, -807713, -807714, -807715 (1–8) can be obtained free of charge from The Cambridge Crystallographic Data Center via www.ccdc.cam.ac.uk/data_request.cif.

Supporting Information (see footnote on the first page of this article): Details of X-ray structure refinement, EDX measurement results, thermogravimetric diagrams, magnetic properties.

Acknowledgments

This work was supported by the Alexander von Humboldt Foundation. Help of Dr. O. Burghaus (EPR spectra), R. Riedel (X-ray data collection), C. Pietzonka (magnetic properties investigation), J. Bamberger (mass spectrometry), M. Hellwig (EDX) and C. Mischke (IR spectra) is gratefully acknowledged.

References

- [1] T. Lis, *Acta Crystallogr., Sect. B* **1980**, *36*, 2042.
- [2] a) D. Gatteschi, R. Sessoli, *Angew. Chem.* **2003**, *115*, 278; *Angew. Chem. Int. Ed.* **2003**, *42*, 268; b) G. Christou, D. Gatteschi, D. N. Hendrickson, R. Sessoli, *MRS Bull.* **2000**, *25*, 66.
- [3] L. Zobbi, M. Mannini, M. Pacchioni, G. Chastanet, D. Bonacchi, C. Zanardi, R. Biagi, U. Del Pennino, D. Gatteschi, A. Cornia, R. Sessoli, *Chem. Commun.* **2005**, 1640.
- [4] a) G. Christou, *Polyhedron* **2005**, *24*, 2065; b) K. V. Shuvaev, L. N. Dawe, L. K. Thompson, *Eur. J. Inorg. Chem.* **2010**, *29*, 4583.
- [5] a) Z. Hassanzadeh Fard, L. Xiong, C. Müller, M. Hołyńska, S. Dehnen, *Eur. J. Chem. Eur. J. Chem.* **2009**, *15*, 6595; b) Z. Hassanzadeh Fard, C. Müller, T. Harmening, R. Pöttgen, S. Dehnen, *Angew. Chem.* **2009**, *121*, 4507; *Angew. Chem. Int. Ed.* **2009**, *48*, 4441; c) M. R. Halvagar, Z. Hassanzadeh Fard, L. Xiong, S. Dehnen, *Inorg. Chem.* **2009**, *48*, 7373; d) Z. Hassanzadeh Fard, M. R. Halvagar, S. Dehnen, *J. Am. Chem. Soc.* **2010**, *32*, 2848.
- [6] a) F. Zonnevillage, M. T. Pope, *J. Am. Chem. Soc.* **1979**, *101*, 2731; b) S. Bareyt, S. Piligkos, B. Hasenknopf, P. Gouzerh, E. Lacote, S. Thorimbert, M. Malacri, *Angew. Chem.* **2003**, *115*, 3526; *Angew. Chem. Int. Ed.* **2003**, *42*, 3404; c) S. Bareyt, S. Piligkos, B. Hasenknopf, P. Gouzerh, E. Lacote, S. Thorimbert, M. Malacria, *J. Am. Chem. Soc.* **2005**, *127*, 6788.
- [7] a) C. J. Milios, A. Vinslava, W. Wernsdorfer, S. Moggach, S. Parsons, S. P. Perlepes, G. Christou, E. K. Brechin, *J. Am. Chem. Soc.* **2007**, *129*, 2754; b) C. J. Milios, R. Inglis, A. Vinslava, R. Bagai, W. Wernsdorfer, S. Parsons, S. P. Perlepes, G. Christou, E. K. Brechin, *J. Am. Chem. Soc.* **2007**, *129*, 12505; c) R. Inglis, L. F. Jones, C. J. Milios, S. Datta, A. Collins, S. Parsons, W. Wernsdorfer, S. Hill, S. P. Perlepes, S. Piligkos, E. K. Brechin, *Dalton Trans.* **2009**, 3403; d) L. F. Jones, M. E. Cochrane, B. D. Koivisto, D. A. Leigh, S. P. Perlepes, W. Wernsdorfer, E. K. Brechin, *Inorg. Chim. Acta* **2008**, *361*, 3420; e) A. Prescimone, C. J. Milios, J. Sanchez-Benitez, K. V. Kamenev, C. Loose, J. Kortus, S. Moggach, M. Murrie, J. E. Warren, A. R. Lennie, S. Parsons, E. K. Brechin, *Dalton Trans.* **2009**, 4858; f) C. J. Milios, C. P. Raptopoulou, A. Terzis, F. Lloret, R. Vicente, S. P. Perlepes, A. Escuer, *Angew. Chem.* **2004**, *116*, 212; *Angew. Chem. Int. Ed.* **2004**, *43*, 210; g) A. Prescimone, C. J. Milios, S. Moggach, J. E. Warren, A. R. Lennie, J. Sanchez-Benitez, K. Kamenev, R. Bircher, M. Murrie, S. Parsons, E. K. Brechin, *Angew. Chem.* **2008**, *120*, 2870; *Angew. Chem. Int. Ed.* **2008**, *47*, 2828; h) C.-I. Yang, K.-H. Cheng, M. Nakano, G.-H. Lee, H.-L. Tsai, *Polyhedron* **2009**, *28*, 1842; i) F. Moro, V. Corradini, M. Evangelisti, V. De Renzi, R. Biagi, U. del Pennino, C. J. Milios, L. F. Jones, E. K. Brechin, *J. Phys. Chem. B* **2008**, *112*, 9729; j) L. F. Jones, C. J. Milios, A. Prescimone, M. Evangelisti, E. K. Brechin, *C. R. Chim.* **2008**, *11*, 1175; k) X. Song, R. Liu, S. Zhang, L. Li, *Inorg. Chem. Commun.* **2010**, *13*, 828; l) R. Inglis, L. F. Jones, C. J. Milios, S. Datta, A. Collins, S. Parsons, W. Wernsdorfer, S. Hill, S. P. Perlepes, S. Piligkos, E. K. Brechin, *Dalton Trans.* **2009**, 3403; m) C. J. Milios, A. Vinslava, W. Wernsdorfer, A. Prescimone, P. A. Wood, S. Parsons, S. P. Perlepes, G. Christou, E. K.

- Brechin, *J. Am. Chem. Soc.* **2007**, *129*, 6547; n) C. J. Milios, R. Inglis, R. Bagai, W. Wernsdorfer, A. Collins, S. Moggach, S. Parsons, S. P. Perlepes, G. Christou, E. K. Brechin, *Chem. Commun.* **2007**, 3476; o) C. J. Milios, R. Inglis, A. Vinslava, R. Bagai, W. Wernsdorfer, S. Parsons, S. P. Perlepes, G. Christou, E. K. Brechin, *J. Am. Chem. Soc.* **2007**, *129*, 12505; p) V. Kotzabasaki, R. Inglis, M. Siczek, T. Lis, E. K. Brechin, C. J. Milios, *Dalton Trans.* **2011**, *40*, 1693.
- [8] a) R. Reshma, P. V. Soumya, S. M. Simi, V. S. Thampidas, R. D. Pike, *Acta Crystallogr., Sect. E* **2009**, *65*, m1110; b) H. Liu, J. Tian, Y. Kou, J. Zhang, L. Feng, D. Li, W. Gu, X. Liu, D. Liao, P. Cheng, J. Ribas, S. Yan, *Dalton Trans.* **2009**, 10511; c) J.-R. Su, L. Zhang, D.-J. Xu, *Acta Crystallogr., Sect. E* **2005**, *61*, m939.
- [9] C. Kozoni, E. Manolopoulou, M. Siczek, T. Lis, E. K. Brechin, C. J. Milios, *Dalton Trans.* **2010**, *39*, 7943.
- [10] S. M. J. Aubin, Z. Sun, H. J. Eppley, E. M. Rumberger, I. A. Guzei, K. Folting, P. K. Gantzel, A. L. Rheingold, G. Christou, D. N. Hendrickson, *Inorg. Chem.* **2001**, *40*, 2127.
- [11] a) C. Ma, Y. Han, R. Zhang, *J. Organomet. Chem.* **2004**, *689*, 1675; b) H.-Q. Hao, H. Zhang, J.-G. Chen, S. W. Ng, *Acta Crystallogr., Sect. E* **2005**, *61*, m1960; c) L. Han, Y. Zhou, S.-J. Huang, *Acta Crystallogr., Sect. E* **2007**, *63*, m455; d) H.-Q. Hao, H. Zhang, *Acta Crystallogr., Sect. E* **2006**, *62*, m30.
- [12] D. Miklos, M. Palicova, P. Segl'a, M. Melnik, M. Korabik, T. Głowiak, J. Mroziński, *Z. Anorg. Allg. Chem.* **2002**, *628*, 2862.
- [13] E. König, in: *Magnetic Properties of Coordination and Organometallic Transition Metal Compounds* (Eds.: K. H. Hellwege, A. M. Hellwege), Springer, Berlin, **1966**, pp. 27–29.
- [14] Stoe & Cie, *X-AREA* (Version 1.54) and *X-RED32* (Version 1.54), Stoe & Cie, Darmstadt, Germany **2002**.
- [15] G. M. Sheldrick, *SHELXTL 5.1*, Bruker AXS Inc., 6300 Enterprise Lane, Madison, WI 53719–1173, USA, **1997**.

Received: December 4, 2011
Published Online: March 8, 2012